[36] J. H. McFee, R. E. Nahory, M. A. Pollack, and R. A. Logan, "Beam deflection and amplitude modulation of 10.6 μm guided waves by free-carrier injection in GaAs-AlGaAs heterostructures," *Appl. Phys. Lett.*, vol. 23, p. 571, 1973.
[37] J. H. McFee, M. A. Pollack, W. W. Rigrod, and R. A. Logan, in *Dig. Tech. Papers, Topical Meeting Integrated Optics* (New Orleans, La.), Jan. 1974.
[38] J. F. Lotspeich, in *Dig. Tech. Papers, Topical Meeting Integrated Optics* (New Orleans, La.), Jan. 1974.
[39] H. L. Garvin *et al.*, "Integrated optics and guided waves—A report of the Topical Meeting," *Appl. Opt.*, vol. 11, p. 1675, 1972.
[40] H. L. Garvin *et al.*, "Ion beam micromachining of integrated optic components," *Appl. Opt.*, vol. 12, p. 455, 1973.
[41] A. Yariv, "Components for integrated optics," *Laser Focus*, Dec. 1972.
[42] J. J. Turner *et al.*, "Gratings for integrated optics fabricated by electron microscope," *Appl. Phys. Lett.*, vol. 23, p. 333, 1973.
[43] A. Y. Cho and F. K. Reinhart, "Growth of three dimensional dielectric waveguides for integrated optics of molecular-beam epitaxy method," *Appl. Phys. Lett.*, vol. 21, p. 355, 1972.
[44] J. C. Tracy, W. Weigman, R. A. Logan, and F. K. Reinhart, "Three-dimensional light guides in single-crystal Ga-As-$Al_xGa_{1-x}As$," *Appl. Phys. Lett.*, vol. 22, p. 511, 1973.
[45] W. H. Louisell, *Coupled Modes and Parametric Electronics*. New York: Wiley, 1960.
[46] S. Somekh, "Theory, fabrication and performance of some integrated optical devices," Ph.D. dissertation, California Inst. Technol., Pasadena, 1974.
[47] A. Yariv, "Coupled-mode theory for guided-wave optics," *IEEE J. Quantum Electron.*, vol. QE-9, pp. 919–933, Sept. 1973.
[48] S. Somekh, E. Garmire, and A. Yariv, "Channel optical waveguiding directional couplers," *Appl. Phys. Lett.*, vol. 22, p. 46, 1973.
[49] S. Somekh *et al.*, "Channel optical waveguides and directional couplers in GaAs-imbedded and ridged," *Appl. Opt.*, vol. 13, p. 327, 1974.
[50] F. K. Reinhart and B. I. Miller, "Efficient GaAs-$Al_xGa_{1-x}As$ modulators," *Appl. Phys. Lett.*, vol. 20, p. 36, 1972.
[51] A. Yariv, *Introduction to Optical Electronics*. New York: Holt, Rinehart and Winston, 1971, p. 326.
[52] H. Stoll, A. Yariv, R. G. Hunsperger, and G. L. Tangonan, "Proton-implanted optical waveguide detectors in GaAs," *Appl. Phys. Lett.*, vol. 23, p. 664, 1973.
[53] H. Stoll, A. Yariv, and R. G. Hunsperger, to be published.
[54] G. E. Stillman, C. M. Wolfe, and I. Melngailis, "Monolithic integrated $In_xGa_{1-x}As$ Schottky barrier waveguide detector," in *Dig. Tech. Papers, Topical Meeting Integrated Optics* (New Orleans, La.), Jan. 1974.
[55] C. M. Wolfe, G. E. Stillman, and I. Melngailis, in *Dig. Tech. Papers, Topical Meeting Integrated Optics* (New Orleans, La.), Jan. 1974.
[56] W. D. Johnston, Jr., and B. I. Miller, "Degradation characteristics of CW $Al_xGa_{1-x}As$ heterostructure lasers," *Appl. Phys. Lett.*, vol. 23, p. 192, 1973.
[57] H. Yonezu *et al.*, "Degradation mechanism of (Al–Ga)As double heterostructure laser diodes," *Appl. Phys. Lett.*, vol. 24, p. 18, 1974.
[58] M. Nakamura, A. Yariv, H. W. Yen, and S. Somekh, "Optically pumped GaAs surface laser with corrugation feedback," *Appl. Phys. Lett.*, vol. 22, p. 515, 1973.
[59] M. Nakamura *et al.*, "Laser oscillation in epitaxial GaAs waveguides with corrugation feedback," *Appl. Phys. Lett.*, vol. 23, p. 224, 1973.
[60] H. Kogelnik and C. V. Shank, "Coupled wave theory of distributed feedback lasers," *J. Appl. Phys.*, vol. 43, p. 2327, 1972.
[61] H. W. Yen *et al.*, "Optically pumped GaAs waveguide lasers with a fundamental 0.11 μm corrugation feedback," *Opt. Commun.*, vol. 9, p. 35, 1973.
[62] M. Nakamura *et al.*, "Liquid phase epitaxy of GaAlAs on GaAs substrates with fine surface corrugations," *Appl. Phys. Lett.*, May 1974. (Similar results were reported at the New Orleans Topical Meeting on Integrated Optics 1974 by Schmidt, Shank, and Miller of Bell Laboratories and by Bannantyne and Tang of Cornell University.)
[63] M. Nakamura, K. Aiki, Jun-Ichi Umeda, A. Yariv, H. W. Yien, and T. Morikawa, "GaAs-$Ga_{1-x}Al_xAs$ double heterostructure distributed feedback diode lasers," *Appl. Phys. Lett.*, vol. 25, pp. 487–488, Nov. 1974.
[64] W. C. Scott, K. L. Lawley, and W. C. Holton, "Mesa surface laser," in *Dig. Tech. Papers, Topical Meeting on Integrated Optics* (New Orleans, La.), Jan. 1974.
[65] M. K. Barnoski, R. G. Hunsperger, and A. Lee, "Ion implanted GaAs injection laser," in *Dig. Tech. Papers, Topical Meeting Integrated Optics* (New Orleans, La.), Jan. 1974.
[66] D. B. Keck, R. D. Maurer, and P. C. Schultz, "On the ultimate lower limit of attenuation in glass optical fibers," *Appl. Phys. Lett.*, vol. 22, p. 307, 1973.

Optical Waveguide Modulators

IVAN P. KAMINOW, FELLOW, IEEE

(Invited Paper)

***Abstract*—A tutorial survey of recent work on optical waveguide modulators in electrooptic, acoustooptic, and magnetooptic materials is presented. Methods for realizing waveguiding layers in modulating materials and various modulator configurations are considered.**

I. INTRODUCTION

HIGH-speed light modulators and beam deflectors that make use of the electrooptic, acoustooptic, magnetooptic, and electroabsorption effects in bulk materials have been described in several reviews [1]–[5]. The first three effects produce refractive index changes in response to the appropriate modulating electric, acoustic, and magnetic fields. The last effect produces a change in optical absorption in response to an electric field.

The performance of these modulators is often specified in terms of μ, the electrical modulating power P required to produce a given degree of modulation over a bandwidth Δf. The performance depends upon optical wavelength λ, the properties of the modulating material, and the device geometry. One of the chief advantages an optical waveguide modulator has over the conventional bulk modulator, is the substantial improvement in the geometrical factor allowed by the confinement of the optical beam to a small cross section over an extended length.

Manuscript received April 19, 1974; revised July 11, 1974.
The author is with the Bell Telephone Laboratories, Crawford Hill Laboratory, Holmdel, N. J. 07733.

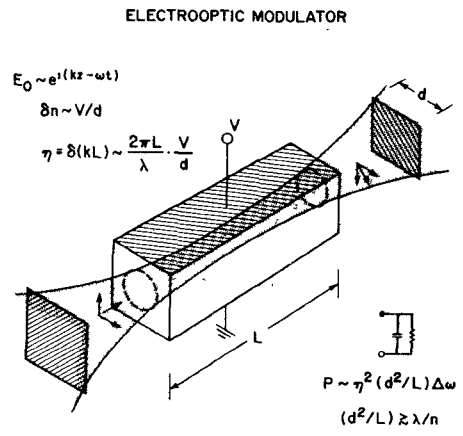

Fig. 1. Focused Gaussian beam passing through a bulk electrooptic modulator rod.

For example, it is easy to show [1] for an electrooptic modulator that

$$\mu \equiv P/\eta^2 \Delta f \sim (hw/L) \tag{1}$$

where η is the phase modulation index. Here we assume that the optical beam completely passes through a volume hwL having cross-sectional dimensions h,w and just containing the modulating field as illustrated in Fig. 1 for $h = w = d$. For a focused Gaussian beam, the minimum value of the geometrical factor is limited by optical diffraction to

$$d^2/L = S^2(4\lambda/\pi n) \tag{2}$$

where n is the refractive index of the electrooptic crystal and S is a factor that is unity when Gaussian spot diameters at the ends of the crystal equal d. In the best practical bulk modulators, S is approximately 3 and μ is about 10 mW/MHz $(\text{rad})^2$ at $\lambda = 1.06$ μm [6]. With optical waveguiding, the diffraction limitation does not apply and, in principle, the geometrical factor can be reduced without limit. Power reduction of 2×10^{-3} below that of a bulk modulator has been predicted for a waveguide modulator at 10.6 μm [7]. Values of μ as low as 0.02 mW/MHz $(\text{rad})^2$ have already been realized at $\lambda = 0.63$ μm [8].

Optical waveguides can be divided into two classes: "planar" waveguides confine the light in one transverse dimension, "strip" guides confine the light in both transverse dimensions. For the strip guide, diffraction does not limit hw/L, but, for the planar guide, the unguided dimension w is still limited by diffraction according to (2) although

$$hw/L = S(4\lambda/\pi n)(h/L^{1/2}) \tag{3}$$

can now be reduced without a diffraction limit by increasing $(L^{1/2}/h)$. However, the corresponding reduction in μ can be realized only if the modulating field is confined to the same volume hwL as that occupied by the optical beam. In later sections, we will describe the various methods that have been studied for making planar and strip waveguides in modulator materials. We consider only single-crystal waveguides of the modulator material itself rather than amorphous or polycrystalline guides on substrates of the modulator crystal because such guides tend to be lossy and/or the interaction tends to be weak. Later, we consider the various electrode configurations that can be employed to provide an efficient interaction between the optical and modulating fields for various purposes such as intensity modulation, deflection, and switching.

It will be seen that strip waveguide modulators and switches can operate with extremely low power when compared with their bulk counterparts. Moreover, they have the potential for being fabricated much more simply and inexpensively. Furthermore, the geometry and size of these devices meet the long-range objective of producing rugged integrated optical circuits. Many important problems still remain before these devices can be applied, e.g., coupling in and out of the modulators, building an efficient PCM modulator, devising a practical multipole switch for single or multimode operation.

II. Optical Waveguide Materials and Modulators

A. Guide Properties

A variety of techniques for producing planar waveguides will be described in later sections. The refractive index profiles in these guides are of two general types: the slab guide, in which the refractive index of the guiding layer is uniform; and the graded-index guide, in which the refractive index of the guiding layer varies throughout its thickness.

The coordinate system for such guides is illustrated in Fig. 2. For the slab guide, Fig. 3(a), the indices of the slab, substrate, and superstrate, respectively, are defined as

$$n_1 > n_2 \geq n_3. \tag{4a}$$

The slab thickness is B and $(n_1 - n_2) = A$.

For the graded-index guide, Fig. 3(b), n_3 is the superstrate index, $n_2 = n_\infty$ is the substrate index for $x \to \infty$ and

$$\begin{aligned} n(x) &= n_\infty + \Delta n(x) \\ \Delta n(\infty) &= 0 \\ \Delta n(0) &= a \\ n(0) &> n_\infty \geq n_3. \end{aligned} \tag{4b}$$

The characteristic layer thickness is taken as b. [See Fig. 3(b).]

The properties of asymmetric slab guides have been treated by many authors [9]. Normalized plots of the propagation constants β_j of the jth TE and TM modes are given in [10]. The number of modes that can propagate in the guide is the integer less than

$$M = \tfrac{1}{2} + (2B/\lambda)(2n_2A)^{1/2}. \tag{5}$$

The wave functions are sinusoidal inside the slab and decay exponentially outside. Sufficiently far from cutoff,

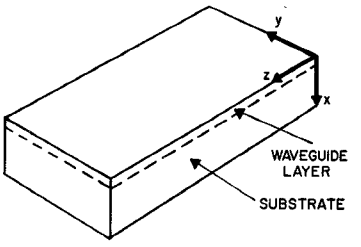

Fig. 2. Coordinate system for planar waveguide.

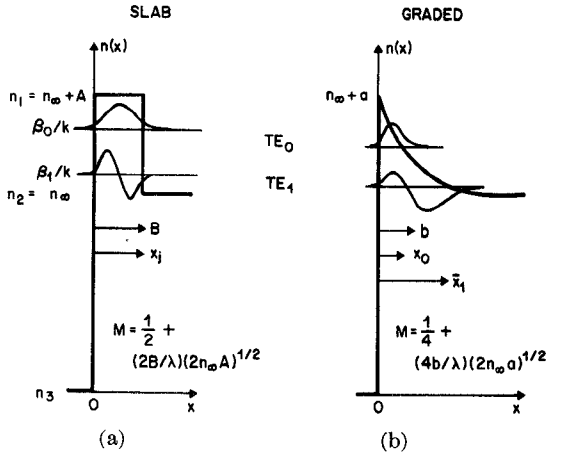

(a) (b)

Fig. 3. Refractive index profiles. (a) Slab. (b) Graded waveguides illustrating wave functions for TE_0 and TE_1 modes. Number of modes M for graded guide is for exponential profile.

which is at $\beta/k = n_2$, most of the optical energy is confined within the slab, $0 < x < B$. Here k is the propagation constant of free space.

For general functions $\Delta n(x)$, the waveguide characteristics of graded-index guides must be found by approximate or numerical methods. However, a useful function that allows analytical solutions [11] of the wave equation and can be used to approximate actual graded-index profiles (see Section II-D) is

$$\Delta n(x) = a_1 \exp(-x/b_1). \tag{6}$$

Normalized plots of the propagation constants for the exponential guide are given in Fig. 4, which is taken from [12] and [13]. The number of modes that can propagate is the integer less than

$$M = \tfrac{1}{4} + (4b_1/\lambda)(2n_\infty a_1)^{1/2}. \tag{7}$$

The wave functions are oscillatory inside the range $0 < x < x_j$ and decay exponentially outside as indicated in Fig. 3(b). Here x_j is the "turning point" for rays of the jth mode, and x_j increases with increasing j. The centroid of energy density is concentrated near x_j and is therefore buried more deeply below the surface for higher order modes. The behavior of rays in multimode slab and graded-index guides are compared in Fig. 5. The turning points for the two cases are B and x_0, x_1, respectively.

A qualitative feel for the behavior of actual guides with more complex $n(x)$ can often be obtained by comparison with those of the slab and exponential guides.

Some applications may call for multimode and others for single-mode waveguides. It is clear from (5) and (7)

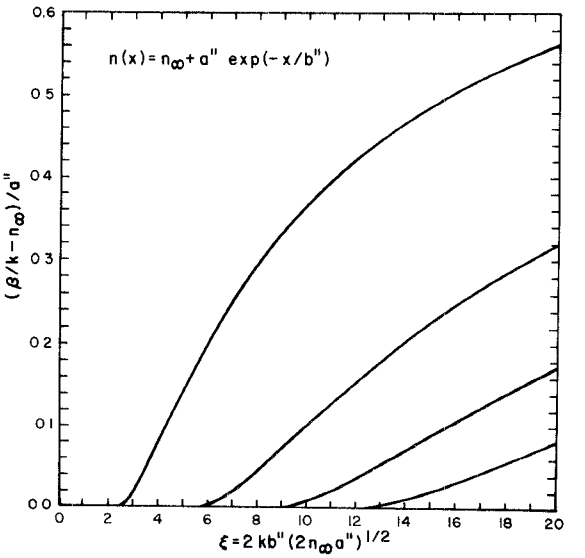

Fig. 4. Normalized phase velocity versus thickness parameter for TE and TM modes of exponential index profile guides [12], [13].

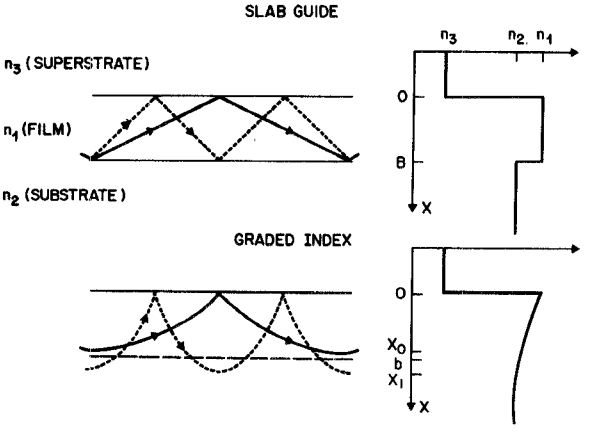

Fig. 5. Ray paths for slab and graded index waveguides illustrating turning points at $x = B$ and $x = x_0, x_1$. The solid and dashed rays represent low and high order modes, respectively.

that for given M the thicknesses, B and b_1, of a guide must vary inversely with the root of the refractive index difference. For surface excitation and surface interaction, thin guides with high index difference are advantageous; for end excitation, low loss, and good mode control, thicker guides with smaller index differences may be desirable.

Most devices will range in length between 1 and 10 mm, and a nominal allowable loss might be 1 dB. Thus guides of practical interest should have less loss than ~1 dB/cm.

B. Plasmon, Schottky Barrier, and p-n Junction Guides

A plasma of free charges (electrons or holes) of density N makes the contribution ΔK to the dielectric constant $K(\omega)$ of a solid, where

$$\Delta K = -\omega_p^2/(\omega^2 + i\omega\tau^{-1}) \tag{8}$$

ω is the applied angular frequency, τ is the collision time, and ω_p is the plasma frequency given by

$$\omega_p^2 = Ne^2/\epsilon_0 n^2 m^* \tag{9}$$

with e the electron charge, ϵ_0 the permittivity of vacuum, n the high-frequency refractive index, and m^* the effective mass. (For $N = 10^{18}$ cm^{-3}, $K = 1$ and m^* the electron mass, we have $\omega_p = 5.7 \times 10^{13}$ s^{-1} and $\lambda_p = 33$ μm.) Thus the free carriers *reduce* the refractive index n,

$$\Delta K/K = 2\Delta n/n \leq 0. \tag{10}$$

Waveguiding layers have been produced in semiconductor materials by reducing the carrier concentration in the guiding layer with respect to the concentration in the substrate. The methods used include proton implantation of the surface of GaAs[14] or GaP[15] to trap some of the carriers, and epitaxial growth of a higher resistivity layer on a low-resistivity substrate [16], [17]. The waveguiding produced is very weak unless N is large; but, then the free carrier absorption, due to the imaginary part of ΔK in (8), makes for a lossy guide. Proton bombardment causes optical loss due to lattice damage; annealing reduces the loss but at the same time restores the carrier concentration.

The resistivity of these semiconductors is usually too low to allow the modulating field to be applied directly; therefore back-biased diode junctions must be employed. Often the modulating field is applied across a Schottky barrier [14], [16] at a metal electrode–semiconductor junction. The width of the barrier should just match the width of the guided mode for efficient interaction. This condition will be satisfied if the resistivity of the guiding layer is very high and that of the substrate very low and if the mode is well confined in the layer. If the resisitvity of the guide is not sufficiently large, the depletion layer will not overlap the guide and the modulation field will interact with just a fraction of the optical mode.

The first optical waveguide modulator made use of a reverse-biased GaP p-n junction [18a]. A back-biased p-n homjunction might be expected to guide because of the reduced carrier concentration in the depletion region and because of the increased refractive index that may be produced by the junction field through the electrooptic effect. In fact, it has been found that the guidance in a p-n junction in GaP is much stronger than can be accounted for by these two mechanisms [18b]. (The true mechanism is not understood.) Even so, because of the relatively small effective index difference, the confinement width of the optical beam exceeds the depletion width containing the modulating field and the overlap is poor. Moreover, the waveguide changes in width and index due to the modulating field thereby introducing nonlinearities [18c]. Some of these problems are alleviated by the use of p-n heterojunctions [see Section II-C-4)].

C. Heteroepitaxial Guides

1) Epitaxial Growth: An ideal epitaxial crystal is a thin layer grown over a bulk single-crystal substrate of the same material. The substrate serves as a template or seed for the location of atoms of the layer so as to continue the structure of the substrate at the interface. The growth material may be supplied in various ways: 1) solution growth—a saturated solution of the material is available at the interface, 2) liquid phase epitaxy (LPE)—a melt of the material is available at the interface, which is held at the crystallization temperature, 3) chemical vapor deposition (CVD)—the component elements are contained in one or more kinds of molecules that are passed over the interface as gases and react there to form the desired compound, 4) molecular beam epitaxy (MBE), evaporation and sputtering—the constituent atoms or molecules are slowly fired at the substrate, which is at a sufficiently high temperature to allow the constituents enough mobility to find their proper places in the lattice, 5) recrystallization—the film material is first deposited on the surface in powdered, polycrystalline, or amorphous form and then heated to the melting point where it forms a single-crystal film using the substrate as a seed. If the interface is a unique natural growth facet of the crystal, the epitaxial overgrowth will be smooth; otherwise, the surface may be rough or characterized by terraces, pyramids, etc. Such surfaces must be polished to reduce scattering in waveguide applications.

The growth of an epilayer on a substrate of the same material is known as *homoepitaxy*. A typical example is Si on Si, which is employed to obtain defect-free silicon with longer minority carrier lifetimes than can be realized in bulk materials. However, for optical waveguide applications we are interested in layers that differ, at least in refractive index, from the substrate. When the composition of the epilayer differs substantially from that of the substrate the process is known as *heteroepitaxy*. Even though the layer and substrate materials differ chemically and optically they may have the same crystal structures and very nearly equal lattice parameters. Then the epitaxy will be similar to homoepitaxy except that the lattice mismatch (on the order of 0.01 Å) is made up over the interface area by elastic strain or by the introduction of lattice defects. The mismatch may be graded over several lattice cells normal to the interface. If the lattice match is poor at the growth or application temperature, one expects strained, cracked, or polycrystalline films. If the structures are totally dissimilar, one expects polycrystalline or amorphous films. In polycrystalline films, the discontinuities at the boundaries between crystallites having dimensions comparable to λ scatter light making for lossy waveguides. In some cases, the polycrystalline film may be partially oriented with a particular axis normal to the interface but with the other axes uncorrelated.

While the preceding discussion may sound reasonable and may even be correct in near ideal instances, epitaxial growth in practice is not well understood. A good review of the present situation is given in [19]. For example, it is found that a (111) Si plane with 3-fold symmetry grows epitaxially on a low-symmetry ($\bar{1}012$) face of sapphire (Al_2O_3) [20]. The lattice match is poor but near—coincidences may occur in certain directions with periods of several unit cells (Moire effect) to provide the epitaxial cues. It is thought that a restructuring of the substrate lattice takes place at the interface transition, which may

extend over a region of thickness greater than 1 μm [20]. The defects in the transition layer influence the electridal properties of these films and might introduce substantial optical losses. A variety of other crystals of unrelated structure have been grown on sapphire, quartz, rock salt, and other readily available crystal substrates.

2) $(NH_4)_\alpha K_{1-\alpha}H_2PO_4$ on KH_2PO_4: KDP (KH_2PO_4) and ADP ($NH_4H_2PO_4$) are well-known water-soluble electrooptic crystals having tetragonal symmetry. Epitaxial films of $(NH_4)_\alpha K_{1-\alpha}H_2PO_4$), 5–75 μm thick, were grown from water solution on {100} planes of a 1.5-cm-long KDP seed [21]. With $\alpha = 0.07$, the film index for both ordinary and extraordinary light is 10^{-3} larger than the substrate index. The lattice mismatches between pure ADP and KDP are 0.05 Å and 0.57 Å for a and c directions, respectively. With $\alpha = 0.07$, the difference is correspondingly reduced. The films are of excellent quality and the losses too small to observe or measure (<1 dB/cm). Unfortunately, the {100} orientation of the film, which has the c axis in the plane, is not suited to modulator applications in crystals of KDP symmetry. Growth on other planes yield undesired {100} and {011} facets.

3) ZnO or AlN on Sapphire: Both ZnO and AlN crystallize in the hexagonal wurtzite structure and are suitable for electooptic or acoustooptic devices.

Hexagonal ZnO layers, 4–10 μm thick, were grown on $(01\bar{1}2)$ sapphire (Al_2O_3) by CVD [22]. The $(11\bar{2}0)$ plane and [0001] direction of ZnO are parallel to $(01\bar{1}2)$ and $[0\bar{1}11]$ of Al_2O_3 so that the c axis of ZnO is in the layer plane, which for ZnO symmetry does allow some modulator applications. However, the resistivity was only 1–10 Ω cm, making it difficult to apply an electric field to the film.

It was necessary to polish the surface in order to reduce the roughness in the as-grown film. These thick films support many modes and the low-order modes, which are far from cutoff, experience loss mainly from the interior of the films while the higher order modes are sensitive to surface roughness. At 0.63 μm, the loss ranges from 5–40 dB/cm as the mode order increases. The low-order mode loss increases as λ^{-4}, indicating that Rayleigh scattering from the interior of the film (rather than resonance absorption) is at fault. The restructured transition region may well be the source of layer scattering centers. Somewhat improved characteristics were reported recently [23].

Single-crystal AlN layers, 0.8–4 μm thick, have been grown on 1-cm-square sapphire substrates by reactive RF sputtering of Al in an NH_4 atmosphere [24]. Films sputtered on (0001) sapphire grow with (0001) planes parallel to the surface while films sputtered on $(01\bar{1}2)$ sapphire grow with $(11\bar{2}0)$ parallel to the surface and the c axis along the $[01\bar{1}\bar{1}]$ axis of sapphire. Optical guiding has not been demonstrated.

4) $Al_\alpha Ga_{1-\alpha}As$ and $Al_\alpha Ga_{1-\alpha}P$ Epilayers and p-n Heterojunctions: Heteroepitaxial films in the GaAs–$Al_\alpha Ga_{1-\alpha}As$ system have been grown by LPE for use in double heterojunction diode lasers [25]. Epilayers for long-lived diode lasers are very sensitive to lattice mismatch. The lattice constants of GaAs and AlAs are nearly identical. Thus the lattice match is nearly perfect for $\alpha = 0.3$. The index of GaAs exceeds that of $Al_\alpha Ga_{1-\alpha}As$ by about 0.45α. A GaAs waveguide layer on $Al_{0.3}Ga_{0.7}As$ will have an index difference of 0.14 and must be extremely thin for single-mode operation. As $\alpha \rightarrow 1$, the bandgap moves from the infrared toward the red ($\sim$0.6 μm).

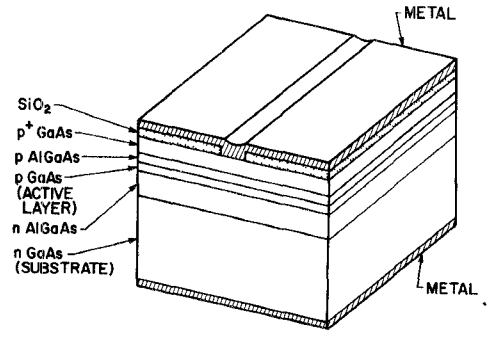

Fig. 6. GaAs–$AlG_\alpha a_{1-\alpha}As$ double heterostructure suitable for p-n junction modulator.

Planar waveguides can be fabricated on a GaAs subsubstrate by first growing a layer of $Al_\alpha Ga_{1-\alpha}As$ and then a layer of GaAs. Compensated layers with high resistivity have not been reported so that these layers are not immediately suited to simple electrooptic application. However, beam deflection and intensity modulation at 10.6 μm have been achieved by exciting photocarriers with a UV pump so as to alter the local plasma frequency [26]. A single layer $Al_\alpha Ga_{1-\alpha}As$ guide on GaAs has also been fabricated by LPE by taking advantage of the natural tendency, due to Al segregation, of α to decrease as the layer thickness grows [27].

However, in order to circumvent the low resistivity of these uncompensated semiconductors, it has been necessary to employ the double heterostructure p-n junction used in laser diodes. Here the GaAs guide layer is sandwiched symmetrically between $Al_{0.3}Ga_{0.7}As$ layers. By suitably doping these layers, a p-n junction can be produced within or at an edge of the guide, so that the depletion region in a back-biased diode overlaps the guided beam. The double heterojunction (DH) structure is illustrated in Fig. 6.

Efficient DH modulators have been demonstrated [28], [29] at $\lambda \sim 1$ μm where a 1-mm-long device requires about 0.1 mW/MHz(rad)^2 with a potential bandwidth of 4 GHz. The thickness of the guiding layer is 0.4–0.9 μm and its effective width (limited by proton-bombardment) is 50 μm. The device is diffraction limited in the plane. Astigmatic lenses are required to couple a circular Gaussian beam into the guide. The coupling introduces substantial insertion loss ($\sim$3 dB). The actual waveguide loss at present is about 8–40 dB/cm, which may not be objectionable for a typical length of 1 mm.

The waveguide supports both TE and TM modes but they are nondegenerate. With suitable crystal orientation the modulator can be made to produce phase modulation of TE and/or TM modes. Amplitude modulation can be achieved in the usual way by exciting both polarizations

(TE and TM) and then recombining them in an external polarizer set at 45° to the junction plane. Since no method is known for introducing a 45° polarizer into the guide, a completely internal amplitude modulator is not feasible. If the TE and TM modes had identical phase velocities, then a crystal orientation could be used such that the principal axes were at ±45° to the plane and a known type TM mode absorber [30] might serve as analyzer.

Quasi-degeneracy can be achieved by reducing the fractional dielectric constant step to ≈ 0.01 [29]. Extinction ratios in excess of 20 dB and characteristic powers near 0.2 mW/MHz for 90-percent intensity modulation should be feasible with $E \parallel (110)$ and $l \approx 1$ mm.

Internal amplitude modulation can be achieved by means of the electroabsorption or Franz–Keldysh effect. It is known that strong electric fields shift the band edge in a semiconductor. Thus the transmission of the waveguide for radiation near the band edge will be modulated by the junction field. A performance of 0.1 mW/MHz for 90-percent intensity modulation has been achieved at $\lambda \sim 0.9$ μm [29]. The effect is large at wavelengths where the quiescent absorption is also large so that efficient electroabsorption devices are intrinsically lossy. However, at 0.9 ρm the quiescent absorption can be made almost negligible [29] with *very clean* material; $\alpha \approx 13$ dB/cm.

Multiple layer DH modulators, grown by LPE, have also been demonstrated in the GaP–$Al_\alpha Ga_{1-\alpha}P$ system [31], which is transparent at 0.633 μm. The index of GaP exceeds that of the $Al_\alpha Ga_{1-\alpha}P$ by 0.45α, much as in the $Al_\alpha Ga_{1-\alpha}As$ case.

5) $LiNbO_3$ on $LiTaO_3$: Lithium niobate is an excellent electrooptic and acoustooptic modulator material. Lithium tantalate, which is an excellent electrooptic but rather poor acoustooptic material, has the same triagonal-crystal structure and similar physical properties as $LiNbO_3$. However, there are several fortuitous differences between their properties: $LiNbO_3$ melts at about 1250°C which is 300°C below the melting point of $LiTaO_3$; the refractive indices, $n_0 \approx 2.29$, $n_e \approx 2.21$, of $LiNbO_3$ at 0.633 μm exceed those of $LiTaO_3$, $n_0 \approx n_e \approx 2.18$; the lattice constant mismatch at room temperature is 0.08 percent and 0.57 percent for a and c, respectively. The last point implies that a good match will occur on a (001) interface at room temperature (but not necessarily at elevated temperatures).

A recrystallized $LiNbO_3$ layer, 6 μm thick, was grown on a (001) LiTaO surface, 10 mm × 15 mm, by spreading a layer of $LiNbO_3$ powder on the surface, heating to 1300°C and cooling slowly [32]. The resultant surface was rough and had to be polished before demonstrating light guiding. Epilayers were also grown on (010) surfaces although some of these tended to crack on the $(10\bar{2})$ cleavage planes of $LiNbO_3$. Since the Curie temperature of $LiTaO_3$ is 600°C, the substrate and film must be poled for modulator applications. A 3-μm thick (010) film guided 1 TE and 3 TM modes at 0.63 μm with losses of ~3 dB/cm [32a)]. Phase modulation was demonstrated using planar electrodes.

A similar method has been used to produce $LiNbO_3$ films on $LiTaO_3$ which are found to have a gradient in composition at the interface [33]. These films are grown on cleavage planes of $LiTaO_3$, which means that the c axis makes an angle of 33° with the plane.

Sputtering has also been used to produce single-crystal layers of $LiNbO_3$ on $LiNbO_3$ or sapphire substrates [34] and $LiNbO_3$ and $LiTaO_3$ layers on $LiNbO_3$, $LiTaO_3$, and fused quartz [35a)]. Waveguiding at 0.63 μm was observed in a $LiNbO_3$ on sapphire crystal with a loss of 9 dB/cm [35b)].

6) $Bi_{12}GaO_{20}$ or $Bi_{12}TiO_{20}$ on $Bi_{12}GeO_{20}$: Bismuth germanate (BGO) and related compounds, obtained by substituting for Ge, form the sillenite family. The crystals belong to the 23-point group which allows optical activity as well as piezoelectricity and a linear electrooptic effect. BGO is a well-known acoustooptic material.

Several members of the family have a larger refractive index and a lower melting point than BGO and give a good lattice match. Films of $Bi_{12}GaO_{20}$ or $Bi_{12}TiO_{20}$ that guide TE and TM modes were obtained by dipping a BGO substrate into a supercooled melt and then lightly polishing the surface [36].

7) Magnetooptic Garnet Films: Yttrium iron garnet (YIG), $Y_3Fe_5O_{12}$, is centrosymmetric, cubic, and ferrimagnetic. Yttrium can be replaced in the lattice by any of the rare earths and by a few other ions such as bismuth, lanthanum, or scandium. The iron can be replaced by gallium or aluminum, in which cases the garnet is no longer ferrimagnetic; yttrium aluminum garnet (YAG) is a well-known laser host. The magnetic garnets exhibit the magnetooptic or Faraday effect whereby the polarization of an optical beam is rotated through an angle θ that is proportional to the product of the optical path length projected onto the magnetization vector $\boldsymbol{M}$ and the Faraday coefficient ρ in degrees/centimeter. A range of θ of ±45°, as the z component of $\boldsymbol{M}$ is switched between the $\pm z$ directions, is required for a magnetooptic switch [3].

The technique of growing epitaxial garnet films by LPE has been developed for magnetic bubble memories. By making complete or partial substitutions on the Y and Fe sites, it is possible to achieve both a good lattice match (0.01 Å) and a higher index waveguide layer on a garnet substrate [37]. The coefficient ρ is large near the absorption edge of the rotation-producing Fe^{3+} ions at about 1 μm but, or course, the optical loss is also large in this region. Impurities also contribute to the absorption. A physical property of practical interest is the rotation per decibel of attenuation at the operating wavelength; for certain special compositions this quantity may be as low as 20°/dB at 1.06 μm according to calculation [38]. The performance of a magnetooptic device is very sensitive to wavelength and, for the iron garnets, the wavelength range is restricted to $\lambda \gtrsim 1$ μm. In a magnetic garnet film of excellent quality on a nonmagnetic substrate the loss, due mainly to absorption, was 8 dB/cm at 1.152 μm [37].

An efficient 1.152-μm thin-film magnetooptic modulator was built by pressing a flat, serpentine modulating elec-

trode against the magnetic film of such a waveguide [39]. The high permeability of the film confines the magnetic field produced by the current through the electrode. As the current is varied, the direction of $\boldsymbol{M}$ is altered so as to vary the coupling between TE and TM modes in the guide via the Faraday effect. The two modes can be discriminated by their polarization or by the angle at which they are coupled from the surface of the film by a prism coupler. Since the TE and TM modes are not synchronous, the pitch of the serpentine electrode is used to make up the phase difference (see Section II-C4). Experimentally, the inductance of the electrode and leads is 0.1 μH and the dc current required to give 52-percent TE–TM conversion is 0.5 A [39]. If 0.1 μH were placed in series with 50 Ω, the bandwidth would be 160 MHz and the modulating power 39 mW/MHz for 52-percent conversion. However, better materials and circuit design could improve the performance appreciably [38]. The actual operation of the thin-film magnetooptic device is analyzed in detail elsewhere [40].

D. Diffused Optical Waveguiding Layers

1) Solid State Diffusion: Diffusion tends to smear a sharp boundary between two media. The thickness of this diffuse region is proportional to $(Dt)^{1/2}$ where D is the diffusion constant and t the diffusion time [41]. The diffusion constant is a strong function of temperature T,

$$D = D_0 \exp(-Q_D/RT), \tag{11}$$

with Q_D the activation energy and

$$R = 1.99 \text{ cal}\cdot\text{mol}^{-1}\cdot\text{K}^{-1} = 8.31 \text{ J}\cdot\text{mol}^{-1}\cdot\text{K}^{-1}.$$

Thus a vapor or an evaporated layer of a substance in contact with the surface of a crystal will diffuse into the crystal to a depth of a few micrometers in a few hours at about 700°C and more quickly at higher T. The diffusing atoms may fill vacancies, or replace atoms, or take up interstitial positions in the crystal [42]. The functional form of the concentration profile after time t depends upon the boundary condition at the surface. For example, if the concentration at the surface is constant with t, then the concentration $c(x,t)$ at depth x is given by the error function complement [41]

$$c(x,t) = c(0,0) \operatorname{erfc}[x/2(Dt)^{1/2}] \tag{12}$$

if the flux, dc/dx, at the surface is constant, then $c(x,t)$ is given by the integral of the error function complement [41]

$$c(x,t) = c(0,0)\pi^{1/2} \operatorname{ierfc}[x/2(Dt)^{1/2}] \tag{13}$$

and, if a limited amount of diffusant is available as a thin surface film, the distribution is Gaussian [42],

$$c(x,t) = \frac{\alpha\tau}{(\pi Dt)^{1/2}} \exp(-x^2/4Dt), \tag{14}$$

where α is the density and τ the thickness of the film initially deposited on the surface.

The impurity atoms may increase the refractive index of the crystal by increasing the polarizability of a unit cell and/or by reducing the volume of the cell. The change in index may be anisotropic, affecting n_0 and n_e differently, depending upon the perturbed configurations of electron bonds formed in the crystal. For the small concentration variations normally encountered, the change in index $\Delta n(x)$ is proportional to $c(x)$. Strains due to changes in lattice parameter will also be small and proportional to $c(x)$. For profiles (12), (13), and (14), respectively, we can take the maximum index changes to be a_2, a_3, and a_4, and the characteristic depths $2(Dt)^{1/2}$ to be b_2, b_3, and b_4 as suggested by (4). Then for these cases,

$$\Delta n(x) = a_2 \operatorname{erfc}(x/b_2) \tag{15}$$

$$\Delta n(x) = a_3\pi^{1/2} \operatorname{ierfc}(x/b_3) \tag{16}$$

$$\Delta n(x) = a_4 \exp(-x^2/b_4^2). \tag{17}$$

The exponential function (6) intersects the functions (15) and (16) at $\Delta n = a_j$, $a_j/2$ and $0 (j = 2,3)$ and approximates them elsewhere when

$$a_1 = a_2 = a_3, \qquad b_1 = 0.69b_2 = 0.51b_3. \tag{18}$$

With these substitutions, the exponential guide characteristics of Section II-A may be used to estimate those of actual guides. The exponential does not provide a very good approximation to the Gaussian profile.

In addition to diffusion of atoms into a solid, one may also diffuse atoms out of a multicomponent solid by a process of "out-diffusion" or "effusion." In this process, the sample is heated in a nonreactive atmosphere and one component evaporates from the surface more readily than the rest [43]. At the same time more of this component diffuses toward the surface in order to reduce the concentration gradient. To good approximation the vaporization flux at the surface is independent of t and (16) holds. The surface layer contains vacancies, which by rearrangement of bonds and/or compression of the unit cell can yield an increased refractive index.

The graded profiles produced by diffusion eliminate much of the scattering due to imperfections and strains at the film substrate boundary in epilayer guides. In addition, the surface quality is often unaffected by the treatment so that repolishing is not required. On the other hand, whereas the index difference A and film thickness B can be controlled independently in epitaxial films, the corresponding a_j and b_j parameters for diffusion are interrelated in some cases and therefore the mode width and mode number cannot be determined separately. An important advantage of in-diffusion is that strip guides can be formed by suitably masking the surface of the crystal during diffusion [44].

2) Diffused Cd(S,Se); Zn(S,Se); (Zn,Cd)Se; and (Zn,Cd)S Layers: The series of 2–6 semiconductors ZnS, ZnSe, ZnTe, CdS, CdSe, CdTe are transparent in the visible, with band edges ranging from about 0.4 μm for ZnS to 0.9 μm for CdTe. The Cd compounds crystallize in the hexagonal wurtzite structure and the Zn compounds often crystallize in the cubic zinc blende structure. These crystals are suitable for electrooptic and acoustooptic applications in the visible and infrared. However, the

materials often have low resistivity and substantial photoconductivity, which leads to space-charge effects that limit their utility in electrooptic applications [45].

In their transparent regions, the refractive indices of the various compounds range between 2.3 and 2.9. Optical waveguiding layers have been produced on a substrate of a low-index crystal by vapor diffusion of either a column 2 or column 6 element. For example, Se has been diffused into CdS to form a guiding layer of $CdSe_\alpha S_{1-\alpha}$ with diffusion depth ~ 3 μm and maximum index change ~ 0.08. Losses at 0.63 μm were about 10–15 dB/cm [46]. Similar guides transparent at 0.63 μm were obtained by diffusing Cd or Se into ZnS, and Cd into ZnSe. Strip guides were produced in Cd-diffused ZnSe by SiO masking to allow the Cd to enter the ZnSe only in a narrow strip. A guide 10 μm deep by 5-mm-long guide had a loss of ~ 3 dB/cm [44]. Strip guides, in both ZnSe and CdS, were used to demonstrate light modulation on a pulsed basis [47]. Coplanar electrodes on the surface alongside the guide, or parallel electrodes above and below the guide provided the fields.

The profile for Cd diffused into ZnSe was measured by observing the photoluminescence spectrum as portions of the surface wave successively etched away [48a)]. Refractive index profiles were measured with a reflection interference microscope [48b)]. The erfc function (15) gave a good representation of the measured profile, and the calculated diffusion constants (11), for $700 < T < 950$°C, were found to be $D_0 = 6.39 \times 10^{-4}$ cm^2·s^{-1}, $(Q_D/R) = 2.17 \times 10^4$K.

3) Out-Diffusion of $LiNbO_3$ and $LiTaO_3$: Both $LiNbO_3$ and $LiTaO_3$ can exist with the stoichiometric lattice structure even with up to 4 percent of the Li sites vacant. As the Li deficiency increases, the extraordinary index increases proportionately but the ordinary index is unaffected. The microscopic origin of this behavior is not understood.

Low-loss waveguides (<1 dB/cm) were made in $LiNbO_3$ or $LiTaO_3$ by heating the crystals above 900°C in vacuum so as to out-diffuse Li_2O [43], [49]. The surface quality is unimpaired by the process. However, $LiTaO_3$, with a Curie temperature of 600°C, becomes depoled while $LiNbO_3$, with a Curie temperature of 1150°C, remains poled. The refractive index profiles for samples treated over a wide range of times and temperatures were measured by observing fringe displacements in an interference microscope. It was found [49] that the ierfc function (16) gave a good representation of the measured profile, and the calculated diffusion constant, which is anisotropic, is given by $D_0 = 3.2 \times 10^{+2}$ and 2.8×10^{-2} cm^2·s^{-1}, $(Q_D/R) = 3.4 \times 10^4$ and 2.5×10^4 K, for $LiNbO_3$ and $LiTaO_3$, respectively, for diffusion normal to the c axis. These studies show that a_3 and b_3 both vary as $t^{1/2}$ and that a_3/b_3 is a very weak function of T. The implications are that a_3 and b_3 cannot be controlled independently by t and T, and that the fundamental mode cannot be confined more closely to the surface than about 12 μm in $LiNbO_3$. This restriction limits applications involving surface interaction and/or surface coupling but may be advantageous in some cases, e.g., the ridge-guide modulator of Section III-F.

Other experiments [50] have shown that similar out-diffusion effects occur in flowing O_2 as well as vacuum; and also that the starting stoichiometry of the substrate has a measurable effect on D. Thus out-diffusion should also work in flowing air, allowing for a very simple out-diffusion apparatus.

Efficient optical phase modulation was demonstrated at 0.63 μm in a planar out-diffused $LiNbO_3$ guide with coplanar electrodes evaporated on the surface [51]. The electrodes were 6 mm long and spaced by 50 μm as required to accommodate diffraction of the beam in the plane. The peak voltage required for 1-rad phase shift is 8 V, the bandwidth is 1.6 GHz, and the modulating power 0.4 mW/MHz(rad)^2.

A surface wave acoustooptic diffraction modulator requiring 250 mW of acoustic power for 100-percent modulation of the zero-order beam was demonstrated at an acoustic frequency of 78 MHz [52a)]. The frequency is limited by the requirement that the optical mode depth, ~ 12 μm, not exceed the acoustic wavelength. A broadband electrooptic Bragg modulator, fabricated in out-diffused $LiNbO_3$, required only 1.6 mW/MHz for 60-percent modulation over a 900-MHz bandwidth [52b)].

The diffraction limitation of the planar electrooptic phase modulator was eliminated in a 1-cm-long ridge waveguide modulator with a dramatic improvement in performance [8]. (See Section III-F.)

4) $LiNb_\alpha Ta_{1-\alpha}O_3$ Guide: It has been found that a metallic layer of Nb ($\sim$500 Å thick) will completely diffuse into a $LiTaO_3$ substrate when heated in an argon atmosphere at 1200°C [53a)]. Since the Curie temperature is 600°C, the crystal must be repoled after treatment. The surface is thought to consist of $LiNb_\alpha Ta_{1-\alpha}O_3$ with α a diffusion function of depth. Single and multimode guides were employed to make an electrooptic Bragg deflection modulator requiring 8-V dc to extinguish the zero-order beam at 0.63 μm. Low-loss single-mode strip guides were made by evaporating Nb through an electron resist mask [53b)]. Guide losses decreased faster than λ^{-4}, approaching ~ 1 dB/cm at 0.63 μm.

5) Metal-Diffused Guides: A wide variety of other metals may be deposited onto $LiNbO_3$ and diffused into the surface at temperatures well below the Curie temperature to produce optical waveguiding layers [53c)]. Typical examples are Ti, V, and Ni. The diffusion profiles are reasonably well described by the Gaussian functions (14) and (16). By adjusting τ, t, and T, one can independently control the number of modes and the effective thickness of the modes. For the Ti-diffused guides with $\tau = 500$ Å, $t = 6$ h, and $T = 950$°C, $b_4 \approx 1$ μm and $a_4 = 0.04$ for extraordinary and 0.01 for ordinary waves. An electrodiffusion technique for producing Cu-doped guides in $LiTaO_3$ was also demonstrated recently [53d)].

Single-mode guides prepared by this in-diffusion process have a significantly smaller diffusion depth than the out-diffused $LiNbO_3$ and $LiTaO_3$ guides. Thus they are better suited to efficient surface interactions. A Ti-diffused $LiNbO_3$ guide was used to make an acoustooptic Bragg deflector with center frequency 175 MHz and bandwidth 30 MHz that requires only 50 mW at electrical and 8 mW of acoustic power for 70-percent deflection [53e].

III. MODULATOR AND DEFLECTOR DESIGN

A. Conventional Intensity Modulators

The electrooptic, acoustooptic, and magnetooptic effects produce refractive index variations that cause phase changes in the optical wave. Most applications require a form of intensity modulation or beam deflection rather than phase modulation. Interference, diffraction, and mode-conversion configurations must be used to adapt the phase modulations for these purposes.

In the usual bulk electrooptic intensity modulator [1]–[3], the incident beam is divided into two orthogonal modes polarized along the principal axes of the modulator crystal. (See Fig. 1.) The applied modulating field does not mix these modes; it merely changes the relative velocities of the modes inducing a phase difference, or retardation, Γ between the modes at the output. When the modes are recombined in a polarizer at $\pm 45°$ to the principal axes the output intensity is given by

$$I = I_0 \cos^2 \Gamma/2 \tag{19}$$

for the output polarizer parallel to the incident polarizer and by

$$I = I_0 \sin^2 \Gamma/2 \tag{20}$$

for the polarizers crossed. If the crystal has natural birefringence, which introduces a fixed Γ_B, a compensator may be employed to cancel it out [6].

The normal modes of a thin-film waveguide are the TE and TM waves, polarized parallel and perpendicular, respectively, to the plane of the film. As a rule, the TE and TM mode velocities differ, even if the film is isotropic, giving rise to an effective Γ_B. At present, we have no polarizer that can be set at 45° to the film plane, although a polarizer set at 0° so as to absorb the TM mode has been demonstrated [30]. Thus a conventional intensity modulator is not now feasible in film form if we insist that all components be integral to the thin-film structure. Of course, there is no problem if conventional compensators and polarizers can be located externally. A different approach is to employ an electrooptic thin-film prism to deflect the beam away from the detector. This method has been demonstrated by passing a 10.6-μm laser beam along the fringing field of the electrode on the surface of an epitaxial GaAs waveguide [17a].

The conventional acoustooptic modulator [4], [5] is based on diffraction or deflection of the optical beam by a bulk acoustic wave. In the thin-film case, it is necessary to employ a surface acoustic wave being certain that the acoustic wave, which is confined within an acoustic wavelength of the surface, closely overlaps the guided optic wave.

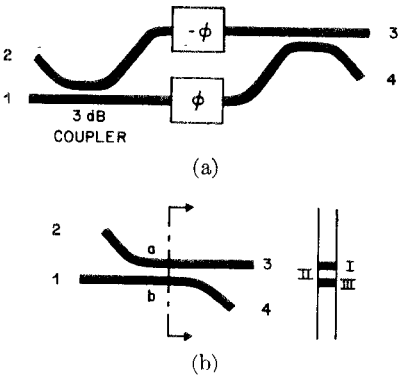

Fig. 7. (a) Balanced bridge modulator/switch. (b) Directional coupler modulator.

The normal modes of a bulk magnetooptic modulator [3] are positively and negatively circularly polarized waves, which unless the TE and TM modes are synchronous, are not normal modes of a film. Thus phase matching must be achieved by introducing a fixed periodicity into the guide. (See Section III-D.)

A few of the techniques for interference, deflection, diffraction, and mode conversion that may be employed in optical waveguides are outlined in the following sections.

B. Balanced Bridge Modulator/Switch

A standard optical means for converting phase change to intensity change is the Mach–Zehnder interferometer; the standard microwave analog is the balanced bridge. The integrated optical circuit adaptation of the microwave bridge is illustrated in Fig. 7(a). Light entering port 1 through a strip guide is equally divided by the 3-dB coupler into the two arms of the balanced bridge. Equal and opposite phase shifts $\pm\phi$ are introduced electrooptically to produce a retardation $\Gamma = 2\phi$ at the output coupler. Then, as in the bulk electrooptic modulator, the outputs at ports 3 and 4 are given by (19) and (20), respectively. The device acts as a reciprocal switch in which energy incident at port 1 may be completely or partially switched between ports 3 and 4 and so on.

Such a device has not yet been demonstrated in optical waveguide form for lack of a 3-dB coupler compatible with strip guide phase modulators. However, the idea has been illustrated with external beam splitters and two planar modulators connected in parallel on the surface of a $LiNbO_3$ crystal with a sputtered polycrystalline niobium oxide guide [54].

C. Directional Coupler Modulator

It is well known from microwave theory that power transfers back and forth periodically between two lossless, coupled waveguides. If β_r and β_s are the propagation constants of the guides and κ is the coupling coefficient, and

if the intensities in guides r and s at $z = 0$ are I_0 and 0, respectively, then [55]

$$I_r(z)/I_0 = 1 - (\gamma + 1)^{-1} \sin^2 (\gamma^2 + 1)^{1/2}\kappa z \quad (21)$$

$$I_s(z)/I_0 = (\gamma^2 + 1)^{-1} \sin^2 (\gamma^2 + 1)^{1/2}\kappa z, \quad (22)$$

where

$$\gamma = \Delta\beta/2\kappa, \qquad \Delta\beta = \beta_r - \beta_s \quad (23)$$

and the length for maximum power transfer is

$$L_0 = \frac{\pi}{2\kappa(\gamma^2 + 1)^{1/2}}. \quad (24)$$

For the phase-matched condition, $\gamma = 0$, the maximum power transfer is unity and $L_0 = \pi/2\kappa$. For a large mismatch, $\gamma^2 \gg 1$, the maximum power transfer is small and L_0 is also small.

Directional coupler modulators that depend upon electrooptic variation of κ or γ have been proposed [55a)]; [56]. One approach is to apply a field to the coupling region II in Fig. 7(b) in order to change κ and L_0. Thus power can be switched completely between ports 3 and 4 if $\Delta\beta = 0$ and if the transfer lengths with and without field, $L_0(E)_m$ and $L_0(0)$, are related by

$$L_0(E)_m/L_0(0) = 2m(m - 1), \qquad m = 1,2,3. \quad (25)$$

Alternatively, equal and opposite fields may be applied to the waveguide regions I and III in order to vary $\Delta\beta$ and L_0 so as to switch power between ports 3 and 4.

Demonstration of these devices awaits the development of a suitable coupler fabrication method. Since the coupler modulator includes both coupling and modulation in one element it may require much tighter tolerances than the bridge modulator in which the coupler and modulator can be optimized separately.

D. Collinear Mode-Conversion Modulators

The modes of a waveguide are orthogonal, i.e., uncoupled, and in general have propagation constants β_j^ρ that differ for each j and polarization ρ (x or y for TE or TM, respectively). A peridic electrooptic, acoustooptic, or magnetooptic perturbation that introduces an off-diagonal element $\Delta n_{\rho\sigma}$, $\rho \neq \sigma$, into the refractive index tensor can couple TE and TM modes propagating in the z direction by destroying the orthogonality. Similarly, the diagonal elements $\Delta n_{\rho\rho}$ can couple either TM or TE modes of different order. Two conditions must be satisfied for power to be transferred between the modes.

1) The spatial variation of $\Delta n_{\rho\sigma}$ along the z direction must contain a Fourier component with period Λ and the temporal variation must contain an angular frequency component Ω such that

$$K = 2\pi/\Lambda = \Delta\beta = \beta_j^\rho - \beta_k^\sigma \quad (26a)$$

$$\Omega = \Delta\omega = \omega_j^\rho - \omega_k^\sigma \quad (26b)$$

where $\Delta\beta$ and $\Delta\omega$ are the differences in propagation constant and angular frequency, respectively, for the two modes. For effective conversion the mismatch $\Delta\beta$ must be less than π/L, where L is the interaction length.

2) The transverse variation of $\Delta n_{\rho\sigma}(x,y)$ must give a nonvanishing overlap integral [9]

$$G = \int_A \Delta n_{\rho\sigma}(x,y) E_j^\rho(x,y) E_k^\sigma(x,y)\, dA \quad (27)$$

where the integration is over the waveguide cross section containing $\Delta n_{\rho\sigma}(x,y)$ and the transverse mode fields E_j^ρ and E_k^σ. The distribution of $\Delta n_{\rho\sigma}(x,y)$ must be sufficiently nonuniform to destroy the orthogonality of the normal modes for nonvanishing G. The coupling coefficient κ is proportional to G. Since the fields are strongest inside the guide, G is larger when the induced index change occurs in the guide rather than in the substrate. Nevertheless, mode conversion can be achieved by modulation of the substrate [57].

Energy must be conserved between the two modes. If they are both guided modes traveling in the same direction, energy is transferred back and forth sinusoidally as in (21) and (22). If Λ is sufficiently small, then energy in a forward traveling wave r may be coupled into a backward wave s according to

$$I_r = I_0 \cosh^2 \kappa(L - z)/\cosh^2 \kappa L \quad (29)$$

$$I_s = I_0 \sinh^2 \kappa(L - z)/\cosh^2 \kappa L, \quad (30)$$

when (26) is satisfied.

The periodic grating may also be employed to couple a guided mode into a mode radiating into the substrate or superstrate at an angle θ from the surface normal. In this case the phase-matching condition (26) holds with β_k^σ replaced by the z component of the radiating wave $n_i k \sin\theta$ with n_i the index of the substrate or superstrate. The energy radiated appears as an attenuation to the guided mode so that [9]

$$I_r = I_0 \exp(-\alpha L). \quad (31)$$

Direct comparisons of the efficiency of guided–guided with guided–radiating mode coupling is not straightforward [9]. However, for given perturbation Δn and coupling length L, the guided–guided interaction is usually stronger because the reduction in I_r is proportional to L^2 rather than L.

A number of periodic mode-coupling modulators in which the coupling can be controlled electrically have been demonstrated. In the magnetooptic modulator [39], the Faraday effect provides TE–TM coupling and the serpentine electrode provides the periodicity ($\Lambda \sim 2$ mm). In another experiment, 55-percent conversion between TE_1 and TE_3 waveguide modes was accomplished by means of an acoustic surface wave [58].

Since $\Delta\beta$ for two forward-traveling guided waves is usually small, the periodicity Λ is generally large and easy to realize. However, forward-to-backward wave coupling requires that $\Delta\beta \sim 2\beta$ and $\Lambda \sim \lambda/2n$. A proposed [59] electrooptic grating modulator may be fabricated by etching or otherwise producing in an electrooptic crystal

a grating tuned to the optical wavelength. Then a modulating electric field E_m applied to the grating can induce an index change Δn causing mismatch

$$\Delta\beta \approx 2\beta\Delta n/n, \tag{32}$$

such that $\Delta\beta > 2\pi/L$, where $2\pi/L$ is the approximate grating bandwidth; then the device will serve as a voltage-controlled shutter that reflects the optical wave for $E = 0$ and transmits it for $E = E_m$ (or vice versa). The device behaves like the Fabry-Perot modulator [1], particularly with respect to bandwidth limitations.

Coupling from a guided to a radiating mode has been proposed [60] and demonstrated [61] acoustooptically. A surface acoustic wave with wavenumber K travels collinearly with a guided optical wave with wavenumber β. Energy is scattered into the substrate with index n_2 at an angle θ with respect to the normal such that

$$kn_2 \sin\theta = \beta - K. \tag{33}$$

By varying the acoustic frequency Ω over the transducer bandwidth $\Delta\Omega$, θ may be scanned through $\Delta\Omega L/2\pi V$ resolvable spots, with V the acoustic velocity. The early experiment with a polystyrene film on quartz substrate waveguide gave a weak acoustooptic coupling [61]. Ti-diffused $LiNbO_3$ has also been used as the acoustooptic medium [62a]. For a 50-MHz bandwidth at 200 MHz, over 100 resolvable spots can be obtained. For a 1-cm interaction length, the access time is $L/V \approx 1.5$ μs. The chief problem, however, is that experimentally [62a] and theoretically [62b] the fraction of guided power coupled out is only $\sim 10^{-5}$ for 200 mW of acoustic power. The coupling coefficient (27) can be improved somewhat by employing a TE_j–TM_k conversion, which reduces the orthogonality of E_j^e and E_k^o over that for TE_j–TE_k or TM_j–TM_k conversion.

A phase grating for collinear interactions may also be produced electrooptically by means of an interdigital electrode of period Λ and length L. However, care must be taken to insure that scattering from the electrode fingers does not produce mode conversion in the absence of the modulating voltage [63]. If the waveguide is sufficiently far from cutoff the optical field at the interdigital electrodes will be small. Alternatively, if, instead of the interdigital electrode, the electrode fingers of opposite polarity lie opposite one another with the optical beam between them, then the optical beam need not pass under the electrodes [64].

Whether a surface acoustooptic or electrooptic grating is used, the modulating fields penetrate less than the period Λ below the surface. The optical mode must then be confined to within the surface by a similar depth for efficient interaction.

E. Bragg and Raman–Nath Diffraction Devices

In the preceding section, the grating vector $\boldsymbol{K}$ was collinear with the incident and scattered wave vectors $\boldsymbol{\beta}_r$ and $\boldsymbol{\beta}_s$. Now we consider cases in which $\boldsymbol{K}$ is nearly normal to $\boldsymbol{\beta}_r$ and $\boldsymbol{\beta}_s$. In these cases, the width L of the grating is

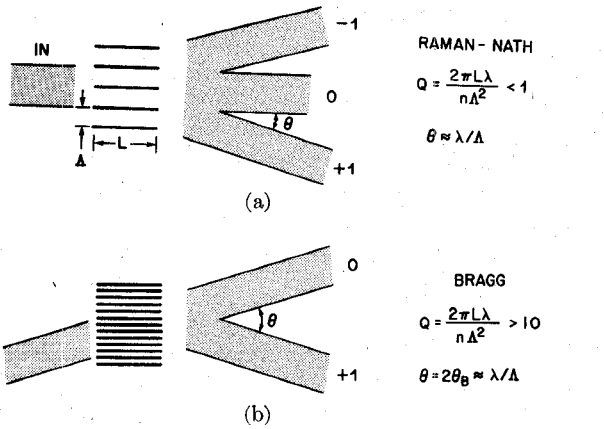

Fig. 8. (a) Raman–Nath. (b) Bragg deflection by thin, $Q < 1$, and thick, $Q > 10$, gratings, respectively.

measured normal to $\boldsymbol{K}$. For normal incidence on a thin grating, part of the beam is transmitted as the zero order and the remainder is diffracted symmetrically into higher order beams at angles θ_m [see Fig. 8(a)] given by

$$m\lambda_g = \Lambda \sin\theta_m, \qquad m = 0, \pm 1, \pm 2, \cdots \tag{34}$$

with guide wavelength

$$\lambda_g = 2\pi/\beta, \tag{35}$$

where we assume $\beta_r = \beta_s = \beta$ for simplicity. The relative energy in the mth order for a sinusoidal grating is

$$I_m/I_0 = J_m^2(\eta) \tag{36}$$

where $J_m(\eta)$ is the Bessel function and the peak phase shift is

$$\eta = 2\pi L\Delta n/\lambda \tag{37}$$

with Δn the peak index change.

The grating is "thin," L is small, when the quantity Q is less than unity; where [65]

$$Q = 2\pi L\lambda/n\Lambda^2, \tag{38}$$

and the diffraction is said to be in the Raman–Nath regime. In this case, a first-order diffracted ray passing through the grating width L is displaced by less than Λ in the $\boldsymbol{K}$ direction and therefore is not reflected by the grating planes.

When Q is large, say $Q > 10$, the diffraction is said to be in the Bragg regime and the diffracted rays experience multiple reflections from many grating periods. In this case, only one diffraction order survives and then only when the Bragg condition

$$\lambda_g = 2\Lambda \sin\theta_B \tag{39}$$

is satisfied [see Fig. 8(b)]. The Bragg angle θ_B is the angle between the incident beam and the normal to K and is twice the angle between the undiffracted and diffracted beams. The intensities in the two beams are, respectively,

$$I_r = I_0 \cos^2(\eta/2) \tag{40}$$

$$I_s = I_0 \sin^2(\eta/2). \tag{41}$$

A unified approach to scattering by a phase grating, including the transition region, $1 < Q < 10$, is given in [65]. Cases in which Bragg diffraction is accompanied by mode conversion, such that $\beta_r \neq \beta_s$, can also be treated in a straightforward manner [66a)] and have been demonstrated for acoustooptic TE_0–TM_0 diffraction [66b)].

As in the previous section, the phase grating may be produced either acoustooptically or electrooptically. The Raman–Nath device may be used to modulate the intensity of the zero-order beam. The Bragg device may serve in addition as a switch and, in the acoustic case with variable frequency, as a scanner. The width L is often limited to approximately 1 cm for compactness and the requirement $Q > 10$ then leads to $\Lambda < 55$ μm for $n = 2$, $\lambda = 1$ μm. In order to insure effective interaction with the fringing field from an interdigital electrode [67] or with a surface acoustic wave, the energy in the optical mode should be within $\sim\Lambda/4$ of the surface. Thus close confinement planar waveguides are required for Bragg devices.

Acoustooptic diffraction has been demonstrated in various waveguide systems: Bragg deflection in glass film sputtered on quartz [68], amorphous AsS_3 sputtered on $LiNbO_3$ [66], amorphous ZnS sputtered on $LiNbO_3$ [69] and Ti-diffused $LiNbO_3$ [53e)], and Raman–Nath diffraction in out-diffused $LiNbO_3$ [52a)]. It is difficult to compare the performance of these devices since various criteria such as operating wavelength, optical loss, modulation efficiency, and bandwidth must be considered. However, the Ti-diffused $LiNbO_3$ Bragg deflector [53e)] required only 50 mW of electrical drive power to produce 70-percent deflection at 0.63 μm over a bandwidth of 30 MHz at 175 MHz.

Electrooptic diffraction has also been demonstrated in several systems: Raman–Nath diffraction in a thin slab of $LiNbO_3$ [70], and Bragg deflection in epitaxial ZnO on sapphire [23], Nb-diffused $LiTaO_3$ [53a)], and out-diffused $LiNbO_3$ [52b)]. The latter device [52b)] employed a low-capacitance electrode configuration, required about 17 V for 65-percent modulation at 900 MHz and 0.63 μm and required 1.6 mW/MHz of bandwidth. A method for producing a single diffracted beam from a series of Raman–Nath gratings with harmonically related periods has also been demonstrated [71].

F. Strip Waveguide Modulators

The devices described so far have operated in planar waveguides. The minimum optical interaction volume is defined by interaction length L in the z direction, the waveguide mode height H in the x direction and the diffraction-limited width W in the y direction. If the modulating field—acoustic, electric, or magnetic—can be confined to the same volume, the interaction will be more efficient than a bulk interaction because L/H can then be increased without a diffraction limit. [See (2)]. A further improvement can be realized in most of the devices, except for the planar Bragg deflector, by introducing guidance in the y direction as well.

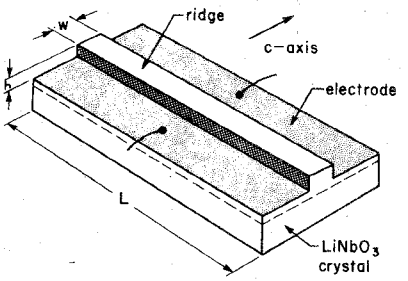

Fig. 9. $LiNbO_3$ ridge waveguide modulator.

Two methods have been demonstrated for producing strip guides in modulating materials: diffusion through a mask and etching away part of a guiding layer to form a ridge guide. In the former experiments [47], Se or Cd were diffused into CdS or ZnSe, respectively, through a SiO_2 mask with a 19-μm-wide aperture. Coplanar electrodes were applied on the surface of the crystal alongside the guide. The fringing field penetrated to a depth about equal to the electrode spacing, $\sim$19 μm, but the waveguide was only 2 μm thick. Therefore the interaction was not as efficient as it might have been had the waveguide cross section been more nearly square, $H \approx W$. A half-wave voltage of 72 V with a rise time less than 5 ns was achieved in one such modulator, on a pulsed basis.

A ridge-guide modulator was produced by ion-beam etching an out-diffused $LiNbO_3$ layer as illustrated in Fig. 9. The ridge was 19 μm wide, 8 μm high, and 11 mm long. Metal electrodes were evaporated alongside and on the walls of the ridge. A 0.63-μm laser beam was injected into the end of the ridge. The guided mode was about 19 μm wide by 9 μm high and was confined within the ridge so that the overlap with the modulating field was excellent. A modulating power of only 20 μW/MHz and a voltage of 1.2 V produced a phase modulation index of 1 rad with a potential bandwidth of 640 MHz.

IV. CONCLUSIONS

The modulators described in Section III represent a considerable advance over the state-of-the-art of four years ago [3]; yet a number of problems remain: If waveguide modulators are to be employed instead of bulk devices because of their efficiency and ease of fabrication, then convenient and efficient coupling methods must be developed. With respect to the various phenomena: The magnetooptic devices only operate in a narrow range of wavelengths near 1 μm; the acoustooptic devices require a high-frequency carrier and have a bandwidth limited by the transducer to about 25 percent of the carrier frequency; the electrooptic device is basically a phase modulator and requires a diffraction or interference configuration to produce intensity modulation. The potential user must examine the known methods and choose the one best suited to his needs given the requirements of wavelength, loss, bandwidth, and power consumption.

Semiconductor laser diodes, because of their short electron and photon lifetimes, can be directly current modulated at bandwidths of a few hundred megahertz [72],

[73]. Although direct modulation is in the early stages of exploration and some difficulties may yet become apparent, it is quite possible that direct modulation of laser and LED diodes will be preferred over external modulation for some moderate bandwidth optical communication applications. However, broadband modulation at wavelengths and power levels not provided by diode lasers still require external modulators. The optical devices discussed here also face strong competition in the switching and display fields from semiconductor and electron beam devices. Thus areas of application of optical waveguide devices depend upon the progress to be realized from the current activity in this new field.

REFERENCES

[1] I. P. Kaminow and E. H. Turner, "Electrooptic light modulators," *Proc. IEEE (A Special Joint Issue on Optical Electronics with Applied Optics, the Optical Society of America)*, vol. 54, pp. 1374–1390, Oct. 1966.

[2] I. P. Kaminow, *An Introduction to Electrooptic Devices*. New York: Academic, 1974.

[3] F. S. Chen, "Modulators for optical communications," *Proc. IEE (Special Issue on Optical Communication)*, vol. 58, pp. 1440–1457, Oct. 1970.

[4] E. K. Sittig, "Elastooptic light modulation and deflection," in *Prog. in Optics*, E. Wolf, Ed., vol. 10. Amsterdam, The Netherlands: North Holland, 1972.

[5] N. Uchida and N. Niizeki, "Acoustooptic deflection materials and techniques," *Proc. IEEE*, vol. 61, pp. 1073–1092, Aug. 1973.

[6] F. S. Chen and W. W. Benson, "A lithium niobate light modulator for optical communications," *Proc. IEEE* (Lett.), vol. 62, pp. 133–134, Jan. 1974.

[7] W. B. Gandrud, "Reduced modulator drive-power requirements for 10.6-μ guided waves," *IEEE J. Quantum Electron.* (Corresp.), vol. QE-7, pp. 580–581, Dec. 1971.

[8] I. P. Kaminow, V. Ramaswamy, R. V. Schmidt, and E. H. Turner, "Lithium niobate ridge waveguide modulator," *Appl. Phys. Lett.*, vol. 24, 1973.

[9] D. Marcuse, *Theory of Dielectric Optical Waveguides*. New York: Academic, 1974.

[10] H. Kogelnik and V. Ramaswamy, "Scaling rules for thin-film optical waveguides," *Appl. Opt.*, vol. 13, 1974.

[11] E. M. Conwell, "Modes in optical waveguides formed by diffusion," *Appl. Phys. Lett.*, vol. 23, p. 328, 1973.

[12] W. Mammel, unpublished.

[13] J. R. Carruthers, I. P. Kaminow, and L. W. Stulz, "Out-diffusion-kinetics and optical waveguiding properties of out-diffused layers in lithium niobate and lithium tantalate," *Appl. Opt.*, vol. 13, p. 2333, 1974.

[14] E. Garmire, H. Stoll, A. Yariv, and R. E. Hunsperger, "Optical waveguiding in proton-implanted GaAs," *Appl. Phys. Lett.*, vol. 21, pp. 87–88, 1972.

[15] M. K. Barnowski, R. G. Hunsperger, R. G. Wilson, and G. Tangonan, "Proton-implanted GaP optical waveguide," *J. Appl. Phys.*, vol. 44, p. 1925, 1973.

[16] a) D. Hall, A. Yariv, and E. Garmire, "Observation of propagation cutoff and its control in thin optical waveguides," *Appl. Phys. Lett.*, vol. 17, pp. 127–129, Aug. 1970.
b) ——, "Optical guiding and electrooptic modulation in GaAs epitaxial layers," *Opt. Commun.*, vol. 1, pp. 403–405, Apr. 1970.

[17] a) P. K. Cheo, "Pulse amplitude modulation of CO_2 laser in an electrooptic thin-film waveguide," *Appl. Phys. Lett.*, vol. 22, p. 241, 1973.
b) ——, "Electrooptic properties of reverse-biased GaAs epitaxial thin films at 10.6 μm," *Appl. Phys. Lett.*, vol. 23, p. 439, 1973.

[18] a) D. F. Nelson and F. K. Reinhart, "Light modulation by the electrooptic effect in reverse biased GaP p-n junctions," *Appl. Phys. Lett.*, vol. 5, p. 148, 1964.
b) F. K. Reinhart, D. F. Nelson, and J. McKenna, "Electrooptic and waveguide properties of reverse-biased gallium phosphide p-n junctions," *Phys. Rev.*, vol. 177, p. 1202, 1969.
c) L. O. Wilson and F. K. Reinhart, "Phase modulation nonlinearity of double-heterostructure p-n junction diode light modulators," *J. Appl. Phys.*, vol. 45, p. 2219, 1974.

[19] I. H. Khan, "The growth and structure of single crystal films," in *Handbook of Thin Film Technology*, L. I. Maissel and R. Glang, Ed. New York: McGraw-Hill, 1970.

[20] C. C. Chang, "Silicon on sapphire epitaxy by vacuum sublimation," *J. Vac. Sci. Technol.*, vol. 8, p. 500, 1971.

[21] V. Ramaswamy, "Epitaxial electrooptic mixed-crystal $(NH_\alpha)_xK_{1-x}H_2PO_4$ film waveguide," *Appl. Phys. Lett.*, vol. 21, p. 183, 1972.

[22] J. M. Hammer, D. J. Chanin, M. T. Duffy, and J. P. Wittke, "Low loss epitaxial ZnO optical waveguides," *Appl. Phys. Lett.*, vol. 21, p. 358, 1972.

[23] J. M. Hammer, D. J. Chanin, and M. T. Duffy, "Fast electrooptic waveguide deflector modulator," *Appl. Phys. Lett.*, vol. 23, p. 1973, 1973.

[24] A. J. Shuskus, T. M. Reeder, and E. L. Paradis, "RF-sputtered aluminium nitride films on sapphire," *Appl. Phys. Lett.*, vol. 24, p. 155, 1974.

[25] M. B. Panish and I. Hayashi, "Heterostructure semiconductor lasers," in *Solid-State Science*, vol. 4, R. Wolfe, Ed. New York: Academic, 1974.

[26] J. H. McFee, R. E. Nahory, M. A. Pollack, and R. A. Logan, "Beam deflection and amplitude modulation of 10.6 μm guided waves by free-carrier injection in GaAs-AlGaAs heterostructure," *Appl. Phys. Lett.*, vol. 23, p. 571, 1973.

[27] E. Garmire, "Optical waveguides in single layers of $Ga_{1-x}Al_xAs$ grown on GaAs substrates," *Appl. Phys. Lett.*, vol. 23, p. 403, 1973.

[28] F. K. Reinhart and B. I. Miller, "Efficient GaAs-$Al_xGa_{1-x}As$ double-heterostructure light modulators," *Appl. Phys. Lett.*, vol. 20, p. 36, 1972.

[29] F. K. Reinhart, "Phase and intensity modulation properties of $Al_yGa_{1-y}As$-$Al_xGa_{1-x}As$ double heterostructure p-n junction waveguides," presented at the Integrated Optics Meeting, New Orleans, 1974.

[30] Y. Suematsu, M. Hakuta, K. Furuya, K. Chiba, and R. Hasumi, "Fundamental transverse electric field (TE_0) mode selection for thin-film asymmetric light guides," *Appl. Phys. Lett.*, vol. 21, p. 291, 1972.

[31] H. P. Kleinknecht and A. E. Widmer, "(GaAl)P optical waveguide modulators fabricated by liquid phase epitaxy," presented at the Integrated Optics Meeting, New Orleans, 1974.

[32] a) S. Miyazawa, "Growth of $LiNbO_3$ single-crystal film for optical waveguides," *Appl. Phys. Lett.*, vol. 23, p. 198, 1973.
b) S. Fukuniski, N. Uchida, S. Miyazawa, and J. Noda, "Electrooptic modulation of optical guided wave in $LiNbO_3$ thin film fabricated by EGM method," *Appl. Phys. Lett.*, vol. 24, p. 424, 1974.

[33] P. K. Tien, S. Riva-Sanseverino, R. J. Martin, A. A. Ballman, and H. Brown, "Optical waveguide modes in single crystalline $LiNbO_3$-$LiTaO_3$ solid solution films," *Appl. Phys. Lett.*, vol. 24, p. 503, 1974.

[34] V. Sadagopan, "Preparation of single crystal films of lithium niobate by radio frequency sputtering," U. S. Patent 3 649 501, Mar. 14, 1972.

[35] a) S. Fukunishi, A. Kawana, and N. Uchida, "Growth and properties of $LiNbO_3$ and $LiTaO_3$ films," *J. Cryst. Growth*.
b) S. Takada, M. Ohnishi, H. Hayakawa, and N. Mikoshiba, "Optical waveguides of single-crystal $LiNbO_3$ film deposited by RF sputtering," *Appl. Phys. Lett.*, vol. 24, p. 490, 1974.

[36] A. A. Ballman, H. Brown, P. K. Tien, and R. J. Martin, "The growth of single crystalline waveguiding thin films of piezoelectric sillenites," *J. Cryst. Growth*, vol. 20, p. 251, 1973.

[37] P. K. Tien, R. J. Martin, S. L. Blank, and S. H. Wemple, and L. J. Varnerin, "Optical waveguides of single-crystal garnet films," *Appl. Phys. Lett.*, vol. 21, p. 207, 1972.

[38] S. H. Wemple, J. F. Dillon, Jr., L. G. VanVitert, and W. H. Grodkiewicz, "Iron garnet crystals for magnetooptic light modulators at 1.06 μm," *Appl. Phys. Lett.*, vol. 22, p. 331, 1973.

[39] P. K. Tien, R. J. Martin, R. Wolfe, R. C. LeCraw, and S. L. Blank, "Switching and modulation of light in magnetooptic waveguides of garnet films," *Appl. Phys. Lett.*, vol. 21, p. 394, 1972.

[40] P. K. Tien, D. P. Schinke, and S. L. Blank, "Magnetooptic and motion of the magnetization in a film-waveguide optical switch," *J. Appl. Phys.*, 1974.

[41] J. Crank, *The Mathematics of Diffusion*. London, England: Oxford, 1970.

[42] P. G. Shewmon, *Diffusion in Solids*. New York: McGraw-Hill, 1963.

[43] I. P. Kaminow and J. R. Carruthers, "Optical waveguiding layers in $LiNbO_3$ and $LiTaO_3$," *Appl. Phys. Lett.*, vol. 22, p. 326, 1973.

[44] W. E. Martin and D. B. Hall, "Optical waveguides by diffusion in II-IV compounds," *Appl. Phys. Lett.*, vol. 21, p. 325, 1972.

[45] I. P. Kaminow, "Measurements of the electrooptic effect in CdS, ZnTe, and GaAs at 10.6 microns," *IEEE J. Quantum Electron.*, vol. QE-4, pp. 23–26, Jan. 1968.

[46] H. F. Taylor, W. E. Martin, D. B. Hall, and V. N. Smiley, "Fabrication of single crystal semiconductor optical waveguides by solid state diffusion," *Appl. Phys. Lett.*, vol. 21, p. 95, 1972.
[47] W. E. Martin, "Waveguide electrooptic modulation in II-IV compounds," *J. Appl. Phys.*, vol. 44, p. 3703, 1973.
[48] a) W. E. Martin, "Photoluminescence determination of Cd diffusion in ZnSe," *J. Appl. Phys.*, vol. 44, p. 5639, 1973.
b) ——, "Refractive index profile measurements of diffused optical waveguides," *Appl. Optics*, vol. 13, p. 2112, 1974.
[49] J. R. Carruthers, I. P. Kaminow, and L. W. Stulz, "Outdiffusion kinetics and optical waveguiding properties of outdiffused layers in lithium niobate and lithium tantalate," *Appl. Opt.*, vol. 13, p. 2333, 1974.
[50] a) N. F. Hartman, R. P. Kenan, P. R. Sievert, C. M. Verber, and V. E. Wood, "Characteristics of diffused waveguiding layers in $LiNbO_3$," presented at the Integrated Optics Meeting, New Orleans, 1974.
b) V. E. Wood, N. F. Hartman, and C. M. Verber, "Characteristics of diffused slab waveguides in $LiNbO_3$," *J. Appl. Phys.*, vol. 45, p. 1449, 1974.
[51] I. P. Kaminow, J. R. Carruthers, E. H. Turner, and L. W. Stulz, "Thin-film $LiNbO_3$ electrooptic light modulator," *Appl. Phys. Lett.*, vol. 22, p. 540, 1973.
[52] a) R. V. Schmidt, I. P. Kaminow, and J. R. Carruthers, "Acoustooptic diffraction of guided optical waves in $LiNbO_3$," *Appl. Phys. Lett.*, vol. 23, p. 417, 1973.
b) J. Noda, N. Uchida, and T. Saku, "Electrooptic diffraction modulator using outdiffused waveguiding layer in $LiNbO_3$," *Appl. Phys. Lett.*, vol. 25, p. 131, 1974.
[53] a) J. M. Hammer and W. Phillips, "Low-loss single-mode optical waveguides and efficient high-speed modulators at $LiNb_xTa_{1-x}O_3$ on $LiTaO_3$," *Appl. Phys. Lett.*, vol. 24, p. 545, 1974.
b) R. V. Schmidt and I. P. Kaminow, "Metal-diffused optical waveguides on $LiNnO_3$," *Appl. Phys. Lett.*, vol. 25, p. 458, 1974.
c) R. D. Standley and V. Ramaswamy, "Nb-diffused $LiTaO_3$ optical waveguides: planar and embedded strip guides," *Appl. Phys. Lett.*, vol. 25, p. 711, 1974.
d) J. Noda, T. Saku, and N. Uchida, "Fabrication of optical waveguiding layer in $LiTaO_3$ by Cu diffusion," *Appl. Phys. Lett.*, vol. 25, p. 308, 1974.
e) R. V. Schmidt and I. P. Kaminow, "Acoustooptic Bragg deflection in $LiNbO_3$ Ti-diffused waveguides," *IEEE J. Quantum Electron.* (Corresp.), vol. QE-11, pp. 57–59, Jan. 1975.
[54] F. Zernike, private communication.
[55] S. E. Miller, "Coupled wave theory and waveguide applications," *Bell Syst. Tech. J.*, vol. 33, p. 661, 1954.
[56] S. Kurazono, K. Iwasaki, and N. Kumagi, "A new optical modulator consisting of coupled optical waveguides," *J. Inst. Electron. Commun. Eng. Jap.*, vol. 55C, p. 103, 1972.
[57] S. Wang, M. Shah, and J. D. Crow, "Studies of the use of gyrostropil and anisotropic materials for mode conversion in thin-film optical-waveguide applications," *J. Appl. Phys.*, vol. 43, p. 1961, 1972.
[58] L. Kuhn, P. F. Heidrich, and E. G. Lean, "Optical guided wave mode conversion by an acoustic surface wave," *Appl. Phys. Lett.*, vol. 19, p. 428, 1971.
[59] I. P. Kaminow and H. Kogelnik, unpublished.
[60] a) W. S. C. Chang, "Acoustooptical deflections in thin films," *IEEE J. Quantum Electron.* (Corresp.), vol. QE-7, pp. 167–170, Apr. 1971.
b) ——, "Periodic structures and their application in integrated optics," *IEEE Trans. Microwave Theory Tech.* (*1973 Symposium Issue*), vol. MTT-21, pp. 775–785, Dec. 1973.
[61] a) F. R. Gfeller and C. W. Pitt, "Collinear acoustooptic deflection in thin films," *Electron. Lett.*, vol. 8, p. 549, 1972.
b) F. R. Gfeller, "Acoustooptic scanner," presented at the Integrated Optics Meeting, New Orleans, 1974.
[62] a) L. Figueroa and I. P. Kaminow, unpublished.
b) D. Marcuse, "Light scattering from periodic refractive index fluctuations in asymmetric slab waveguides," *IEEE J. Quantum Electron.*, to be published.
[63] I. P. Kaminow, W. Mammel, and H. P. Weber, "Metal-clad optical waveguides: Analytical and experimental study," *Appl. Opt.*, vol. 13, p. 396, 1974.
[64] I. P. Kaminow, unpublished.
[65] W. R. Klein and B. D. Cook, "Unified approach to ultrasonic light diffraction," *IEEE Trans. Sonics Ultrason.*, vol. SU-14, pp. 123–134, July 1967.
[66] a) Y. Ohmachi, "Acoustooptical light diffraction in thin films," *J. Appl. Phys.*, vol. 44, p. 3928, 1973.
b) Y. Ohmachi, "Acoustooptic TE_0–TM_0 mode conversion in a thin-film of amorphous tellurium dioxide," *Electron. Lett.*, vol. 9, p. 539, 1973.
[67] H. Engan, "Excitation of elastic surface wave eaves by spatial harmonics of interdigital transducers," *IEEE Trans. Electron Devices*, vol. ED-16, pp. 1014–1017, Dec. 1969.
[68] L. Kuhn, M. L. Dakss, P. F. Heidrich, and B. A. Scott, "Deflection of an optical guided wave by a surface acoustic wave," *Appl. Phys. Lett.*, vol. 6, p. 265, 1970.
[69] R. V. Schmidt, unpublished.
[70] M. A. R. P. deBarros and M. G. F. Wilson, "High speed electrooptic diffraction modulator for baseband operation," *Proc. Inst. Elec. Eng.* (London), vol. 119, p. 807, 1972.
[71] S. Wright and M. G. F. Wilson, "New form of electrooptic deflector," *Electron. Lett.*, vol. 9, p. 169, 1973.
[72] T. L. Paoli and J. E. Ripper, "Direct modulation of semiconductor lasers," *Proc. IEEE* (*Special Issue on Optical Communication*), vol. 58, pp. 1457–1465, Oct. 1970.
[73] M. Chown, A. R. Goodwin, D. F. Lovelace, G. H. B. Thompson, and P. R. Selway, "Direct modulation of double-heterostructure lasers at rates up to 1 Gbit/s," *Electron. Lett.*, vol. 9, p. 34, 1973.

Nonreciprocal Magnetooptic Waveguides

JOHN WARNER

Abstract—**The longitudinal magnetooptic effect can be used in a unique way to mix TE and TM modes of a planar dielectric waveguide where the strength of mixing is dependent upon propagation direction (forwards or reverse). A detailed study of Faraday effect circulators in optical dielectric waveguides is presented and accurate design data for a practical version are offered. At this writing, experimental confirmation has been hampered by lack of success in optically contacting two dissimilar materials.**

Manuscript received March 21, 1974; revised July 8, 1974. This work was supported in part by the Advanced Research Projects Agency, ARPA Order 2327 and is published by permission of Her Brittanic Majesty's Stationary Office.

The author was with the U. S. Naval Research Laboratory, Washington, D. C. He is now with the Royal Radar Establishment, Malvern, Worcs., England.

I. INTRODUCTION

THE development of integrated optics is still at the stage where experiments on components for detection, modulation, and switching are being reported. We would like to add to these reports with our detailed study of how